Iron-Loaded Synthetic Chrysotile: A New Model Solid for Studying the Role of Iron in Asbestos Toxicity

ARTICLE *in* CHEMICAL RESEARCH IN TOXICOLOGY · APRIL 2007

Impact Factor: 3.53 · DOI: 10.1021/tx600354f · Source: PubMed

13 AUTHORS, INCLUDING:

Elena Gazzano
Università degli Studi di Torino
42 PUBLICATIONS **835** CITATIONS
SEE PROFILE

Elisabetta Aldieri
Università degli Studi di Torino
42 PUBLICATIONS **1,092** CITATIONS
SEE PROFILE

Giorgio Lesci
LEBSC srl
57 PUBLICATIONS **773** CITATIONS
SEE PROFILE

Chiara Riganti
Università degli Studi di Torino
90 PUBLICATIONS **1,853** CITATIONS
SEE PROFILE

Iron-Loaded Synthetic Chrysotile: A New Model Solid for Studying the Role of Iron in Asbestos Toxicity

Elena Gazzano,[†,#] Francesco Turci,[‡,#] Elisabetta Foresti,[§] Maria Grazia Putzu,[⊥,#] Elisabetta Aldieri,[†,#] Francesca Silvagno,[†] Isidoro Giorgio Lesci,[§] Maura Tomatis,[‡,#] Chiara Riganti,[†,#] Canzio Romano,[⊥,#] Bice Fubini,[‡,#] Norberto Roveri,[§] and Dario Ghigo*[,†,#]

Dipartimento di Genetica, Biologia e Biochimica, Università di Torino, Via Santena 5/bis, Italy, Dipartimento di Chimica IFM, Università di Torino, Via P. Giuria 7, Italy, Dipartimento di Chimica "G. Ciamician", Università di Bologna, Via Selmi 2, Italy, Dipartimento di Traumatologia, Ortopedia e Medicina del Lavoro, Università di Torino, Via Zuretti, 29, Italy, and Interdepartmental Center "G. Scansetti" for Studies on Asbestos and Other Toxic Particulates, Università di Torino, Italy

Received December 18, 2006

The generation of reactive oxygen species and other radicals, catalyzed by iron ions at the fiber surface, is thought to play an important role in asbestos-induced cytotoxicity and genotoxicity, but a direct confirmation of this statement needs the availability of asbestos samples differing only for their iron content, without the interference of other physicochemical features. Synthetic stoichiometric chrysotile nanofibers, devoid of iron or any other contaminant, did not exert genotoxic and cytotoxic effects nor elicited oxidative stress in a murine alveolar macrophage cell line; on the contrary, the same nanofibers, loaded with 0.57% and 0.94% (w/w) iron, induced DNA strand breaks, lipoperoxidation, inhibition of redox metabolism and alterations of cell integrity, similarly to natural chrysotile. On the other hand, the incubation with ferric nitrilotriacetate, a cell-permeating iron complex, even if it caused an intracellular overloading of iron very similar to that elicited by iron-loaded synthetic chrysotile and by natural chrysotile, did not exert any of these effects. This suggests that chrysotile is not toxic by acting simply as a carrier of iron into the cell, but rather that the redox activity of iron is potentiated when organized at the fibers surface into specific crystallographic sites having coordination states able to activate free radical generation. Synthetic chrysotile fibers may be proposed as a standard reference sample and model solids for experimental studies on asbestos fibers aiming to clarify the mechanisms of its toxicity and to synthesize new fibers devoid of pathogenic effects.

Introduction

Epidemiologic and animal studies indicate that inhalation of asbestos fibers can result in pulmonary interstitial fibrosis (asbestosis), bronchogenic carcinoma, pleural plaques, and malignant mesothelioma (*1*). The molecular mechanisms underlying the fibrogenic and tumorigenic effects of asbestos are not yet fully established; different physicochemical factors have been involved, mainly related to the fibrous habit and to surface reactivity (*1*−*4*). Iron is a stoichiometric component (about 27%, w/w) in amphiboles such as crocidolite $[Na_2(Fe^{2+},Mg^{2+})_3(Fe^{3+})_2Si_8O_{22}(OH)_2]$ and amosite $[(Fe^{2+},Mg)_7Si_8O_{22}(OH)_2]$, while in natural chrysotile $[Mg_3Si_2O_5(OH)_4]$ it is a contaminant (about 1−6%, w/w), replacing isomorphously magnesium and silicon (*2*, *5*, *6*). Experimental evidence suggests that the generation of reactive oxygen species and other radicals, catalyzed by iron ions at the fiber surface, plays an important role in asbestos-induced cytotoxicity and genotoxicity (*7*, *8*). Antioxidants and iron chelators have been shown to attenuate asbestos-induced cytotoxicity in macrophages, pulmonary epithelial cells, mesothelial cells, and endothelial cells (*2*). Furthermore, DNA strand break formation appears related to the presence of iron on the fibers (*9*), and iron chelators decrease the asbestos-induced DNA damage (*10*). Yet, the role played by iron in asbestos pathogenicity is still a matter of debate (*8*, *10*, *11*). In previous reports, to prove the role of iron in their toxicity, asbestos fibers have been either depleted or enriched in iron with different procedures (*2*), which may also change some structural and surface properties of the fibers, introducing further variables in the study.

Chrysotile nanofibers, fully devoid of iron and any other contaminating metal ion, have been recently synthesized in hydrothermal conditions as a unique phase, with definite structure, morphology, and stoichiometric composition (*12*, *13*). We have previously observed that these synthetic fibers, opposite to Rhodesian chrysotile (UICC A, Union Internationale Contre le Cancer[1]), do not exert cytotoxic effects and do not induce oxidative stress in human lung A549 epithelial cells (*14*). Iron, which is usually contained as contaminant in the natural and not in the stoichiometric synthetic chrysotile, could be responsible for such a difference, but natural and synthetic chrysotile fibers also differ in micromorphology, size distribution of the fiber, and presence of contaminants other than iron. More recently, synthetic chrysotile nanofibers loaded with a controlled amount of iron (0.57% and 0.94% w/w, respectively) have been

* Corresponding author. Phone: +39-011-6705849. Fax: +39-011-6705845. E-mail: dario.ghigo@unito.it.
† Dipartimento di Genetica, Biologia e Biochimica, Università di Torino.
‡ Dipartimento di Chimica IFM, Università di Torino.
§ Università di Bologna.
⊥ Dipartimento di Traumatologia, Ortopedia e Medicina del Lavoro, Università di Torino.
Interdepartmental Center "G. Scansetti" for Studies on Asbestos and Other Toxic Particulates, Università di Torino.

[1] Abbreviations: 6PGD, 6-phosphogluconate dehydrogenase; FeNTA, ferric nitrilotriacetate; G6PD, glucose 6-phosphate dehydrogenase; LDH, lactate dehydrogenase; MDA, malonyldialdehyde; PPP, pentose phosphate pathway; UICC A, Union Internationale Contre le Cancer.

10.1021/tx600354f CCC: $37.00
Published on Web 02/22/2007

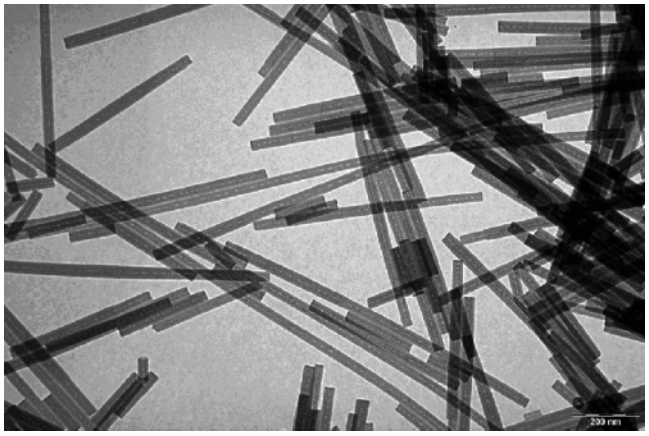

Figure 1. TEM image of synthetic chrysotile nanofibers loaded with 0.57% (w/w) iron, showing the hollowed tubular structure and the concentrically arranged "cylinder in cylinder" morphology and exhibiting outer diameters of 20 ± 2 (single-cylinder morphology) and 50 ± 3 nm (two-cylinders morphology) and lengths ranging from 500 nm to 2 μm. The same morphology is exhibited by the synthetic chrysotile nanofibers devoid of iron or containing 0.94% (w/w) iron (not shown).

prepared with the same synthesis method. They exhibit the same features—structure, size, tubular morphology, and exposed surface—of the corresponding iron-free nanofibers (*15*). To get direct evidence of the role of iron in asbestos toxicity we have compared the ability of synthetic chrysotile (both stoichiometric and loaded with iron) and ferric nitrilotriacetate, a cell-permeating iron complex, to cause DNA strand breaks, oxidative stress, and cell damage in the murine alveolar macrophage cell line MH-S, investigating whether these effects could be related to the simple cellular loading with iron.

Materials and Methods

Materials and Cells. Stoichiometric chrysotile nanofibers (Figure 1) devoid of iron or containing controlled amounts of the metal (0.57% and 0.94%, w/w) have been synthesized as previously described (*12*, *13*, *15*). UICC A chrysotile, which contains 2.14% (w/w) Fe^{3+} ions (measured as Fe_2O_3) and 0.41% (w/w) Fe^{2+} ions (measured as FeO), was used as a positive control (*16*). When not otherwise specified, reagents were purchased from Sigma-Aldrich S.r.l. (Milan, Italy). A solution of 1 mM ferric nitrilotriacetate (FeNTA) was prepared by mixing 1:1 2 mM nitrilotriacetic acid (NTA) in 1 N NaOH and 2 mM ferric chloride in 1 N HCl; the pH was adjusted at about 7 with NaOH (*17*). Murine alveolar macrophages MH-S, provided by Istituto Zooprofilattico Sperimentale "Bruno Ubertini" (Brescia, Italy), were cultured in RPMI-1640 + 10% fetal bovine serum up to confluence, and then incubated for 24 h in either the absence or presence of UICC A or synthetic chrysotile fibers before the assays. All chrysotile samples were sonicated (Labsonic sonicator, 100 W, 10 s) before incubation with cells, to dissociate fiber bundles and allow better suspension and diffusion in the culture medium; this procedure does not modify the physicochemical characteristics of the fibers (data not shown). The protein content of cell monolayers and cell lysates was assessed with the BCA kit from Pierce (Rockford, IL). The amount of intracellular iron after incubation under different experimental conditions was assessed by an inductively coupled plasma (ICP) spectrometer (Perkin-Elmer Optima 4200 DV; Perkin-Elmer, Shelton, CT). After a 24 h incubation in the absence or presence of UICC A chrysotile, synthetic stoichiometric chrysotile, synthetic chrysotile loaded with 0.94% iron, or FeNTA, MH-S cells were washed with fresh medium, detached with trypsin/EDTA, washed with PBS, resuspended at 1×10^6 cells/mL in 1 mL of PBS, and sonicated on ice with two 10 s bursts. The amount of iron was measured in the cell lysate using an ICP and expressed as μg of iron/mg of cell proteins (Figure 2). MitoTracker red CM-H_2XRos

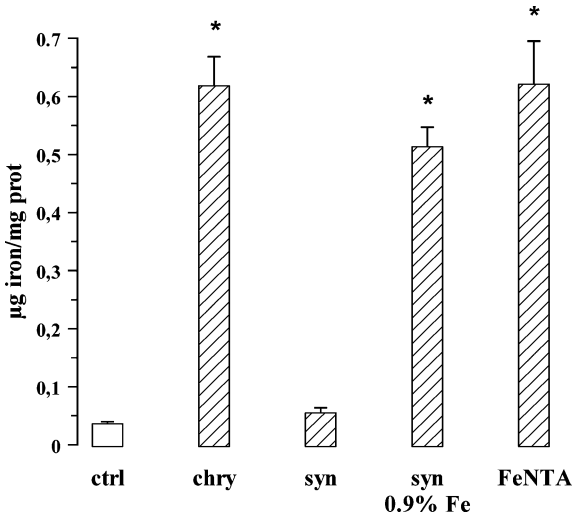

Figure 2. Intracellular content of iron in MH-S cells incubated for 24 h in the absence (ctrl) or presence of 6 μg/cm^2 UICC A chrysotile (chry), synthetic stoichiometric chrysotile (syn), synthetic chrysotile loaded with 0.94% iron (syn 0.9% Fe), or 1 μM ferric nitrilotriacetate (FeNTA). Measurements were performed in duplicate by ICPMS (see Materials and Methods), and data are presented as means ± SEM (n = 3). Vs. control: $p < 0.0001$.

and 2′,7′-dichlorodihydrofluorescein diacetate (DCFH-DA) were purchased from Molecular Probes, Invitrogen (Carlsbad, CA).

Alkaline Comet Assay. Single-cell gel electrophoresis (comet assay) was performed under alkaline conditions according to the method of Singh et al. (*18*) with slight modifications. All steps were conducted under dim yellow light to prevent additional DNA damage. A 7.5 μL cell suspension (5×10^4 cells) was mixed with 75 μL of low melting point agarose (0.8%) and placed on the clear part of a frosted microscope slide precoated with a layer of normal melt point agarose (1%) and low melting point agarose. Then, slides were immersed in lysis buffer for 1 h (4 °C, 2.5 M NaCl, 0.1 M Na_2EDTA, 10 mM Tris, 0.5% *N*-laurylsarcosine, supplemented with 1% Triton X-100 just before use). To perform the DNA unwinding, slides were placed in a horizontal electrophoresis unit containing the electrophoresis buffer (300 mM NaOH, 1 mM Na_2EDTA, pH > 13) for 40 min. Alkaline electrophoresis was performed in the same buffer for 20 min (25 V, 300 mA). Slides were washed three times with neutralization buffer (0.4 M Tris, pH 7.5), and then they were dehydrated in 70% ethanol (5 min) and left to dry, allowing storage until analysis. To analyze DNA damage, slides were stained with DAPI (10 μg/mL, 5 min). Fifty randomly chosen, nonoverlapping comets per comet slide were observed using a Leica fluorescence microscope (20× objective) and an image analysis system (CometScore, TriTek Corp. U.S.A.).

Lactate Dehydrogenase (LDH) Leakage. After a 24 h incubation, the extracellular medium was centrifuged at 12 000*g* for 15 min to pellet cellular debris, whereas cells were washed with fresh medium, detached with trypsin/EDTA, washed with PBS, resuspended at 1×10^5 cells/mL in 0.2 mL of 82.3 mM triethanolamine phosphate hydrochloride (pH 7.6), and sonicated on ice with two 10 s bursts. LDH activity was measured in the extracellular medium and in the cell lysate, using a Lambda 3 spectrophotometer (Perkin-Elmer, Shelton, CT), as previously described (*19*), to check the cytotoxic effect of chrysotile (*20*). Extracellular LDH activity was calculated as percentage of total LDH activity of each dish.

Measurement of Malonyldialdehyde (MDA). After a 24 h incubation, cells were washed with fresh medium, detached with trypsin/EDTA, and resuspended in 1 mL of PBS. Lipid peroxidation was spectrophotometrically detected with a Packard EL340 microplate reader (Bio-Tek Instruments, Winooski, VT) measuring the intracellular level of MDA, the end product derived from the breakdown of polyunsaturated fatty acids and related esters, with the lipid peroxidation assay kit (Oxford Biomedical Research, Oxford, MI), which uses the reaction of *N*-methyl-2-phenylindole

with MDA in the presence of hydrochloric acid to yield a stable chromophore with maximal absorbance at 586 nm (*21*).

Measurement of Intracellular Glutathione. GSH was measured as described by Vandeputte et al. (*22*), using a glutathione reductase−Ellman reagent recycling assay and an EL340 microplate reader (Bio-Tek Instruments).

Measurement of Pentose Phosphate Pathway (PPP) Activity. The metabolic flux through the PPP was measured as previously described (*23*), by subtracting the amount of CO_2 developed from [6-^{14}C]glucose from the CO_2 released from [1-^{14}C]glucose (Dupont−New England Nuclear, Boston, MA) in 1 h, in the absence or presence of an oxidative stress (menadione, 100 μM).

Measurement of Glucose 6-Phosphate Dehydrogenase (G6PD) and 6-Phosphogluconate Dehydrogenase (6PGD) Activities. Cells were washed with fresh medium, detached with trypsin/EDTA, washed with PBS, resuspended at 0.1×10^6 cells/mL in 0.1 M Tris/0.5 mM EDTA pH 8, and sonicated on ice with two 10 s bursts. This cell lysate was checked for the activity of G6PD and 6PGD using a Lambda 3 spectrophotometer (Perkin-Elmer), as previously described (*23*).

Free Radical Generation (Fenton Activity and Homolytic Cleavage of C−H Bonds). The release of hydroxyl (HO•) and carboxylate (CO_2•$^-$) radicals was detected by electron paramagnetic resonance (EPR), by means of the spin-trapping technique with 5-5′-dimethyl-1-pirroline-*N*-oxide as trapping agent, as previously described (*24*, *25*).

Transmission Electron Microscopy Analysis. Transmission electron microscopy images were obtained using a Philips TEM CM100 (Philips, Eindhoven, The Netherlands). Samples were suspended in doubly distilled water and sonicated for 2 min in order to disaggregate the particles, without any additional treatment. A drop of the chrysotile suspension was transferred onto holey carbon foils supported on conventional copper microgrids.

Detection of Production of Reactive Oxygen Species (ROS) by Confocal Scanning Laser Microscopy. MH-S cells were grown to confluence in 8-well chambered coverslips (Nunc, Rochester, NY) and incubated with 6 μg/cm^2 natural and synthetic chrysotile (UICC A chrysotile, synthetic chrysotile, synthetic chrysotile loaded with 0.94% iron) for 24 h or with 500 μM H_2O_2 for 15 min (used as a positive control). After these incubation times, cells were loaded for 15 min with 10 μM DCFH-DA and 0.2 μM MitoTracker red. DCFH-DA is cleaved intracellularly by nonspecific esterases to form DCFH, which is further oxidized by ROS to form the fluorescent compound dichlorofluorescein (DCF). MitoTracker red is a red-fluorescent dye that stains mitochondria in live cells and whose accumulation is dependent upon membrane potential. After this further incubation cells were washed and observed under a Leica DM IRE2 inverted microscope equipped with a PL APO 63×/1.32−0.6 oil immersion objective and a Leica TCS SP2 laser scanning microscope system (Leica, Heidelberg, Germany) equipped with Ar UV, ArKr, and HeNe lasers. Intracellular ROS generation was detected as DCF fluorescence (excitation, 488 nm; emission, 500−550 nm), whereas mitochondrial organelles were stained by MitoTracker red fluorescence (excitation 543 nm; emission 590−700 nm). Colocalization of fluorescence was given by the merged yellow signal. The effect of DCFH photo-oxidation was minimized by collecting the fluorescence image with a single rapid scan (line average 2, total scan time 3 s), and identical parameters were used for all determinations.

Statistical Analysis. All data in text and figures are provided as means ± SEM. Results were analyzed by a one-way analysis of variance and Tukey's test (software: SPSS 11.0 for Windows, SPSS Inc., Chicago, IL).

Results and Discussion

After a 24 h incubation in the absence or presence of different samples of chrysotile, MH-S cells were subjected to single-cell gel electrophoresis (comet assay) (Table 1). Three indexes of DNA damage were recorded: tail length (measured from the middle of the comet to the end of the tail), tail DNA (percentage of DNA in the tail), and tail moment (= tail length × tail DNA). All these indexes were significantly higher in MH-S cells incubated with UICC A chrysotile in comparison with cells incubated in the absence of fibers. The parameters of DNA damage were not modified in control cells incubated with iron-free synthetic chrysotile, while they appeared significantly increased in cells incubated with synthetic chrysotile loaded with 0.57% and 0.94% iron (Table 1). In order to clarify whether chrysotile-associated iron is per se responsible for DNA strand breaks, under the same experimental conditions we incubated MH-S cells with FeNTA, a compound able to hold iron in a soluble form also at neutral or alkaline pH and to increase the intracellular iron content bypassing the transferrin receptor (*17*). In our experimental conditions, a cell culture dish incubated with 1 μM FeNTA contains the same absolute amount of iron as that carried by 6 μg/cm^2 iron-loaded (0.94% w/w) chrysotile fibers. More important, after a 24 h incubation of MH-S cells with 1 μM FeNTA the intracellular content of iron significantly increased, exhibiting a value very similar to that observed after a 24 h incubation with 6 μg/cm^2 UICC A chrysotile and iron-loaded (0.94% w/w) chrysotile (Figure 2). In spite of this, 1 μM FeNTA did not induce any significant change on the indexes of DNA damage in comparison with the control, even when added to the cell cultures together with iron-free chrysotile (Table 1). A solution of 10 μM FeNTA was ineffective as well (Table 1).

Table 1. Tail Length, Tail DNA, and Tail Moment Obtained from Comet Assays Performed on MH-S Cells Incubated for 24 h in the Absence (Control) or Presence of 6 μg/cm^2 UICC A Chrysotile, Synthetic Chrysotile, Synthetic Chrysotile Loaded with 0.57% or 0.94% (w/w) Iron, or 1−10 μM FeNTA[a]

	tail length (μm)	tail DNA (%)	tail moment
control	17.4 ± 0.8	1.9 ± 0.1	0.4 ± 0.0
UICC A chrysotile	115.1 ± 5.6**	13.2 ± 2.4**	3.2 ± 0.5**
synthetic chrysotile (no iron)	22.8 ± 1.6	1.5 ± 0.1	0.3 ± 0.0
synthetic chrysotile (0.57% iron)	65 ± 2.9**	7.8 ± 1.5*	1.4 ± 0.2*
synthetic chrysotile (0.94% iron)	82.5 ± 3.2**	10.8 ± 2.2*	1.6 ± 0.2*
FeNTA (1 μM)	17.6 ± 1.2	1.8 ± 0.2	0.5 ± 0.1
FeNTA (1 μM) + synthetic chrysotile (no iron)	18.2 ± 1.1	2.0 ± 0.2	0.4 ± 0.3
FeNTA (10 μM)	19.8 ± 1.5	1.9 ± 0.1	0.5 ± 0.2

[a] Data are presented as means ± SEM from three experiments; at least 50 cells were evaluated in each experiment. Vs. control: * $p < 0.001$; ** $p < 0.0001$.

After a 24 h incubation with natural and iron-loaded chrysotile, a decrease of intracellular levels of GSH (the main cellular antioxidant compound) was observed in MH-S cells (Figure 3). On the other hand, the incubation with iron-free synthetic chrysotile did not induce depletion of GSH levels.

Furthermore, after the incubation with UICC A chrysotile and iron-loaded chrysotile, MH-S cells exhibited a significant increase of LDH release, an index of cytotoxicity (*20*), and MDA accumulation, a product of lipoperoxidation (*21*) (Figure 4). The presence of exogenous GSH prevented these effects, suggesting that the cell damage evoked by these particulates is due to an oxidative stress. On the contrary, iron-free synthetic chrysotile did not modify significantly LDH release and MDA accumulation (Figure 4). Incubation of cells with FeNTA (1 and 10 μM), in the absence or presence of iron-free chrysotile, did not change these parameters in comparison with control or iron-free chrysotile alone, respectively (not shown).

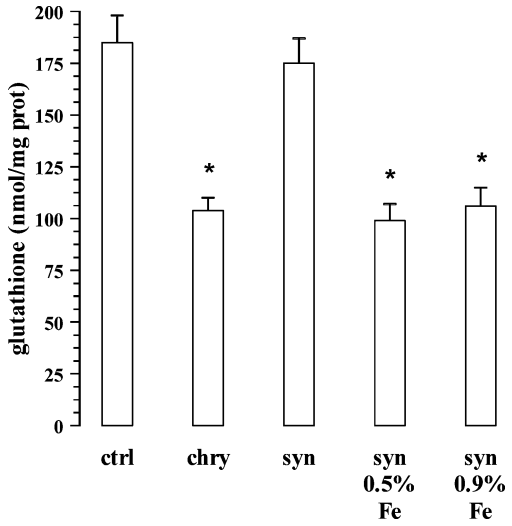

Figure 3. Intracellular levels of glutathione (GSH) in MH-S cells incubated for 24 h in the absence (ctrl) or presence of 6 μg/cm^2 UICC A chrysotile (chry), synthetic chrysotile (syn), or synthetic chrysotile loaded with 0.57% iron (syn 0.5% Fe) or 0.94% iron (syn 0.9% Fe). Extracellular GSH and intra- and extracellular glutathione disulfide were also measured (*21*); each significant decrease of intracellular GSH was accompanied by a parallel increase of the sum of their values (not shown). Measurements were performed in duplicate, and data are presented as means ± SEM ($n = 8$). Vs. control: $* p < 0.0001$.

Iron ions exposed at the surface of asbestos are associated with the potential to trigger two independent mechanisms of free radicals generation: hydroxyl (HO•) radicals (via a Fenton reaction) and carbon-centered free radicals (via homolytic rupture of a carbon−hydrogen bond) (*3*). Using EPR, we have investigated with the spin-trapping technique the potential of our samples to release HO• and $CO_2^{\bullet -}$ radicals in a solution containing H_2O_2 or sodium formate, respectively. Fenton activity was absent in the iron-free chrysotile but sustained up to more than 1 h with both FeNTA and the iron-loaded fibers, already at the lowest iron charge (0.57%) (Figure 5A). In the absence of ascorbic acid, no EPR signal from carbon-centered radicals was detected with each fiber type and with FeNTA (not shown). In fact, as a consequence of the spontaneous oxidation in contact with air, iron is present as ferric ion in both FeNTA and at the fiber surface, and it is known that Fe(III) is able to generate hydroxyl radicals but not carbon-centered radicals (*25*). Some of us have previously observed that ascorbic acid, once in contact with crocidolite asbestos fibers (*25*) and other particulates (*26*, *27*), reduces iron at the fiber surface, allowing the radical generation to take place. The presence of a large variety of reducing biomolecules, such as ascorbic acid, in human tissues makes it feasible that such an activation of the fiber surface may virtually occur in any biological compartment. For instance, ascorbic acid is present in the fluid lining the respiratory airways and can interact with asbestos fibers after inhalation (*28*). When in the presence of ascorbic acid, a clear carbon-centered radical generation was observed from iron-loaded synthetic chrysotile samples, already at the lowest iron charge available (0.57%) (Figure 5B), but neither from the iron-free one nor, interestingly, from FeNTA. This suggests that, in a reducing environment like the cell, iron is able to elicit the generation of carbon-centered radicals only when poorly coordinated at the chrysotile surface, while iron entering the cell as a chelate of NTA is not able to trigger such a radical production even under reducing conditions. It is noteworthy that the FeNTA complex has a much higher stability constant (*29*) than the corresponding one with ascorbate (*30*).

Both in cellular tests and in the cell-free system, we did not find significant differences between the effects of fibers containing 0.57% and 0.94% iron. This means that low amounts of metal, like those found to contaminate natural chrysotile, are largely enough to elicit a significant cell damage in murine alveolar macrophages. A similar response pattern, in terms of LDH, MDA, and GSH levels, has been observed in the human lung A549 epithelial cells incubated under the same experimental conditions (not shown).

These results suggest that iron is necessary for synthetic chrysotile to induce genotoxic (DNA strand breaks) and cytotoxic (release of LDH activity) effects at an extent similar to that observed in cells treated with the natural form of chrysotile. These signs of cell damage are likely to be dependent on an oxidative stress, since they are accompanied, under the same experimental conditions, by an increase of the lipoperoxidation product MDA and a decrease of intracellular GSH. Furthermore, iron-loaded synthetic nanofibers can cause the generation of free radicals in a cell-free system.

Recent experimental evidence has demonstrated that amosite and crocidolite asbestos fibers cause apoptosis of human alveolar epithelial cells and rat pleural mesothelial cells by inducing mitochondrial dysfunction and mitochondrial DNA damage (*31*, *32*). The alteration of functional electron transport may result in mitochondrial-derived ROS production that in turn mediates cells apoptosis (*33*). We checked the origin of ROS in our experimental conditions by confocal scanning laser microscopy experiments. To evaluate the ROS production into mitochondria and/or cytosol, we double-stained cells with the ROS-sensitive fluorescent probe DCFH and the fluorescent marker of mitochondria MitoTracker red (Figure 6). As expected, we observed a significantly increased ROS generation versus controls only in cells incubated with either UICC A chrysotile or iron-loaded synthetic chrysotile; in these cells the ROS production was intense, similar to that observed in presence of H_2O_2, and ubiquitous. ROS were detectable both in cytosol and mitochondria (as evidenced by the merged signal yellow). Cells treated with synthetic iron-free chrysotile did not show significant differences when compared with controls. Our data are not in contrast with recent observations made by other groups (*31*−*33*), since, although those studies collectively indicate that mitochondria are initial targets of asbestos-induced DNA damage and apoptosis via an oxidant-related mechanism, the contribution of different cell compartments to ROS generation is still matter of debate and investigation. Confocal scanning laser microscopy results confirm the central role played by iron in the free radicals generation induced by fibers of natural and synthetic chrysotile.

We have previously shown that crocidolite (*23*), amosite (*34*), and chrysotile (*14*) asbestos inhibit the antioxidant metabolic route PPP which provides cells with the NADPH required to maintain GSH in its reduced form. This inhibition is mediated by the impairment of the activity of G6PD, the rate-limiting enzyme of PPP. We have already shown that purified G6PD is inhibited by asbestos fibers via an oxidative damage, since the enzyme activity is protected by GSH (*34*). To assess whether their inhibition is mediated by fiber-associated iron, we measured both PPP and G6PD activity in MH-S cells after a 24 h incubation with or without the different types of chrysotile fibers. As well as natural chrysotile, iron-loaded synthetic fibers induced an inhibition of PPP and G6PD, without changing the activity of 6PGD, another enzyme of PPP (Figure 7). The effect on PPP was more evident when PPP was maximally activated by the oxidizing agent menadione (Figure 7A). Menadione

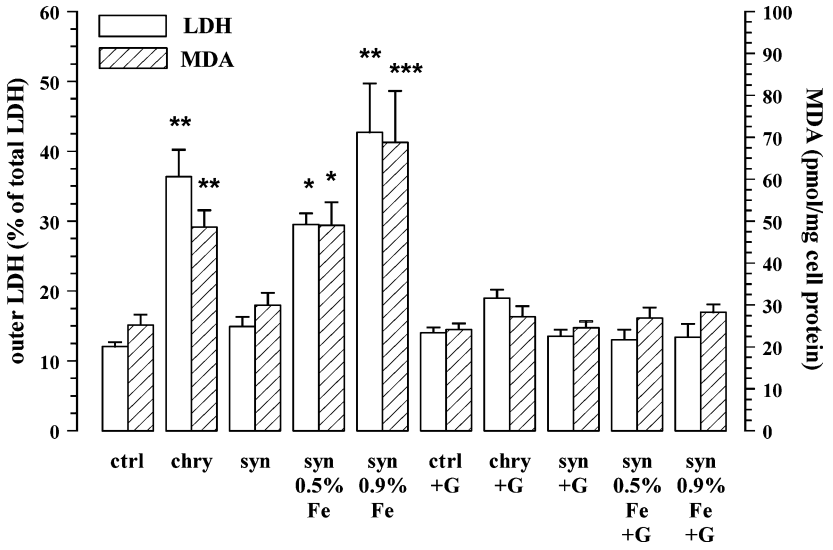

Figure 4. Extracellular release of lactate dehydrogenase (LDH) and accumulation of intracellular malonyldialdehyde (MDA) in MH-S cells incubated for 24 h in the absence (ctrl) or presence of 6 μg/cm^2 UICC A chrysotile (chry), synthetic chrysotile (syn), or synthetic chrysotile loaded with 0.57% iron (syn 0.5% Fe) or 0.94% iron (syn 0.9% Fe) and in the absence or presence of 10 mM GSH (G). Measurements were performed in duplicate, and data are presented as means ± SEM ($n = 8$). Vs. control: $* p < 0.03$; $** p < 0.001$; $*** p < 0.0001$.

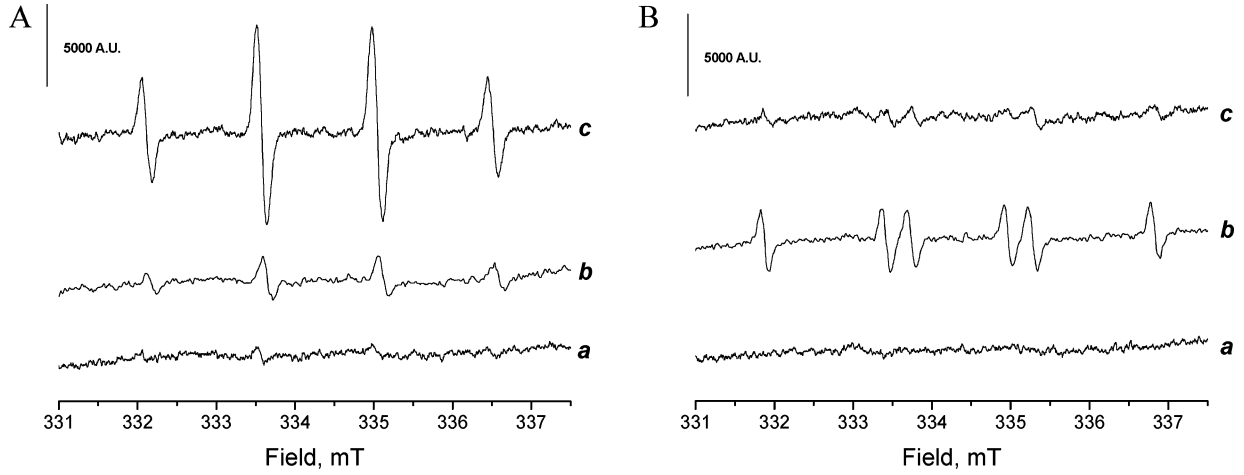

Figure 5. EPR spectra of the adducts of hydroxyl (HO•) (A) and carboxylate ($CO_2^{\bullet -}$) radicals (B) with the spin-trapping agent 5-5′-dimethyl-1-pirroline-*N*-oxide. HO• radicals released upon incubation of either 10 mg of fibers or 10 mM FeNTA with a H_2O_2 solution (0.08 mM) and $CO_2^{\bullet -}$ radicals generated in a buffered solution of sodium formate (2 M) containing either 10 mg of fibers or 10 mM FeNTA were detected by means of a spin-trapping technique, as previously described (*23*). The pH was kept at 7.4. The kinetics of the free radical yield was followed for at least 1 h. The number of radicals released is proportional to the intensity of the EPR signal. The extraction of the hydrogen atom from the formate ion to generate $CO_2^{\bullet -}$ was performed in the presence of 1.5 mM ascorbic acid (*24*). Blanks were made by operating in the same way but in the absence of fibers. All spectra were recorded on a Miniscope MS 100 (Magnettech, Berlin, Germany) spectrometer at a microwave power level of 10 mW, middle of range 3375 G, scan range 120 G, and a modulation amplitude of 1 G. All the experiments were repeated at least twice. In both figures signal a has been obtained in a suspension of iron-free synthetic chrysotile, signal b from a suspension of iron-loaded (0.57%) synthetic chrysotile, in the same experimental conditions. Signal c was obtained in the presence of 10 mM FeNTA solution. Each figure is representative of three experiments with similar results. Chrysotile loaded with a higher content of iron (0.94%) exhibited a signal superimposable to the b tracing of both panels (not shown).

induces oxidative stress and subsequent PPP activation by generating superoxide anion through its redox cycling and by forming a conjugate with glutathione (*35*). The oxidative stress induced by asbestos fibers has a different origin. Chrysotile (*14*) and other types of asbestos fibers (*23, 34*) exert their cytotoxic effects not only by generating high amounts of ROS, but also by inhibiting the PPP antioxidant cycle. We have already shown that the PPP blockage is, at least partly, mediated by the inhibition of G6PD (*23*, *34*). The present study confirms previous results, and furthermore it provides the new evidence that the inhibitory effect of asbestos on PPP and G6PD depends on the iron content of fibers.

When the effects of fibers on PPP flux and G6PD activity are compared, the decrease of PPP activity was more evident than the decrease of G6PD activity. This discrepancy can be explained by the different meaning of the two measurement procedures. PPP flux is strictly related to in vivo G6PD activity and is measured under the intracellular concentrations of reagents, which are low and not saturating, so that the G6PD rate is far from Vmax. G6PD activity is measured in lysed cells in the presence of saturating concentrations of reagents, then the enzyme rate matches Vmax. Furthermore, G6PD has been demonstrated to operate normally at a rate that is a small fraction (0.05−2%) of its Vmax (*36*); this so-called "restraint" is a common feature of G6PD from all somatic cells. The cell lysis, performed to measure the G6PD Vmax, removes the restraining factors and unmasks a vast reserve of enzyme activity. In whole cells the effect of asbestos can be observed only on the small part of G6PD which supports PPP, while in broken cells it is detectable on the total amount of G6PD. For these reasons the

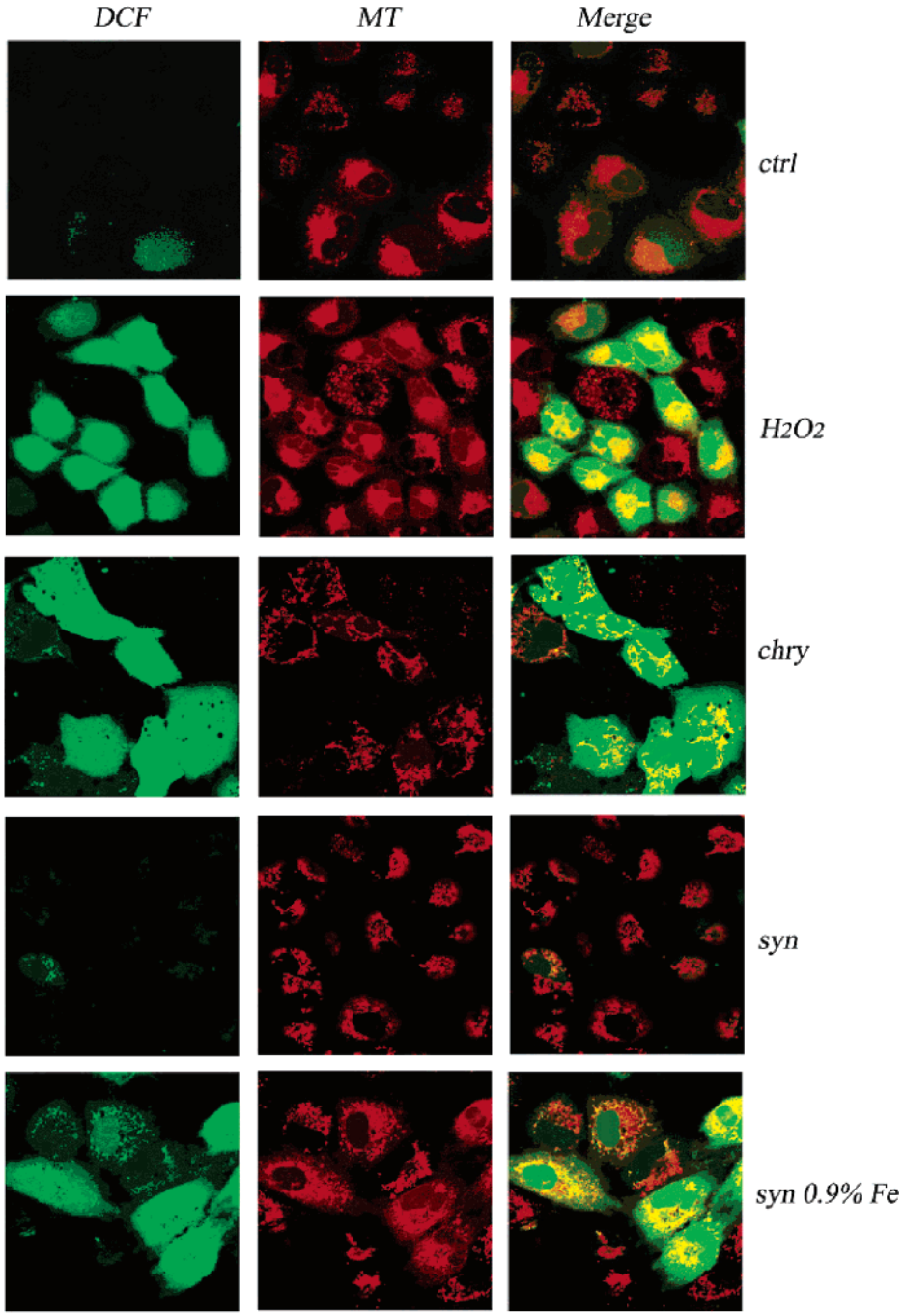

Figure 6. Effect of chrysotile fibers on intracellular ROS production in MH-S cells. Cells were incubated for 24 h in the absence (ctrl) or presence of 6 μg/cm^2 UICC A chrysotile (chry), synthetic chrysotile (syn), or synthetic chrysotile loaded with 0.94% iron (syn 0.9% Fe). Aliquots of control cells were treated for 15 min with 500 μM hydrogen peroxide (H_2O_2). The cells were then incubated with 10 μM dichlorodihydrofluorescein diacetate (DCF) and 0.2 μM MitoTracker red (MT) for 15 min before being imaged by confocal scanning laser microscopy (see Materials and Methods). Left to right: DCF fluorescence (green), MitoTracker fluorescence (red), and merged image (yellow). Each figure is representative of three experiments with similar results.

PPP measurement is a more sensitive index of the asbestos effect on the actual antioxidant defense potential of the cell (*23*). Incubation of cells with 1 and 10 μM FeNTA, in the absence or presence of iron-free chrysotile, did not modify significantly PPP (both basal and stimulated by menadione) and G6PD activity in comparison with control or iron-free chrysotile alone, respectively (not shown).

It has been supposed that asbestos fibers are toxic since they act as passive "carriers" of iron into the cells; being phagocytosized, fibers would bypass the control exerted by the transferrin receptor, causing an intracellular iron overload and subsequent iron-catalyzed Fenton reaction with generation of radical species (*37*). We think that this mechanism is not fully consistent with several experimental evidences. For instance, any simple oxidative stress is expected to activate PPP; on the contrary, we have observed that exposure to asbestos fibers inhibits PPP (*14*, *23*, *34*), suggesting a more complex effect of asbestos on cell redox metabolism. Furthermore, when we incubated MH-S cells with a 1 μM dose of the cell-permeating iron complex FeNTA, containing as much iron as the total iron contained in iron-loaded (0.94%) nanofibers (6 μg/cm^2) and producing a similar iron cellular overload, no sign of oxidative stress and genotoxic and cytotoxic effects was observed in comparison with that of controls. This result is more intriguing if we consider

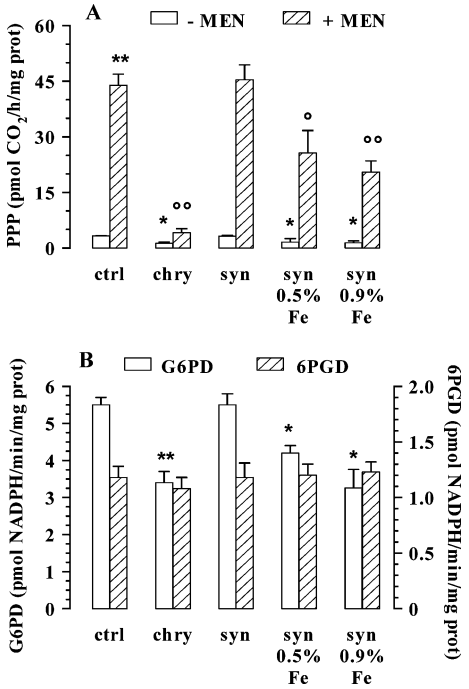

Figure 7. Effect of chrysotile fibers on pentose phosphate pathway (PPP) (panel A) and on the activity of glucose 6-phosphate dehydrogenase (G6PD) and 6-phosphogluconate dehydrogenase (6PGD) (panel B) in MH-S cells incubated for 24 h in the absence (ctrl) or presence of 6 μg/cm2 UICC A chrysotile (chry), synthetic chrysotile (syn), or synthetic chrysotile loaded with 0.57% iron (syn 0.5% Fe) or 0.94% iron (syn 0.9% Fe). (A) After the incubation period, cells were washed, detached, and checked for PPP activity, in the absence (−MEN) or presence (+MEN) of 100 μM menadione, as described under Materials and Methods. Measurements were performed in duplicate, and data are presented as means ± SEM ($n = 5$). Vs. control −MEN: $* p < 0.01$; $** p < 0.0001$. Vs. control +MEN: $° p < 0.001$; $°° p < 0.0001$. (B) After the incubation period, cells were washed, detached, lysed, and checked for G6PD and 6PGD activity, as described under Materials and Methods. Measurements were performed in duplicate, and data are presented as means ± SEM ($n = 8$). Vs. control: $* p < 0.02$; $** p < 0.0001$.

that only iron at the fiber's surface (which represents a minor part of the total iron in the fiber bulk) is assumed to react with biomolecules and generate free radicals in cell-free experiments (*34*, *38*); this means that cells were exposed to more freely reactive iron when incubated with 1 μM FeNTA than with iron-loaded nanofibers. Even 10 μM FeNTA was devoid of significant toxic effects. FeNTA is known to induce DNA damage (*39*) and lipoperoxidation (*40*), by inducing intracellular iron overload, both in vivo and in vitro, and the subsequent generation of reactive oxygen species via a Fenton mechanism. In in vitro experiments, to induce these effects FeNTA is generally incubated at 40−100 μM or more (see, for instance, refs *41*−*43*). We too had observed, in a first set of experiments, that 150 μM FeNTA induces in MH-S cells a toxic effect and oxidative stress (measured as LDH release and MDA accumulation) very similar to those observed with natural and iron-loaded chrysotile (not shown). We have used much lower concentrations of FeNTA in the experiments described here, and this is the likely reason why the iron complex did not induce per se a toxic effect.

Taken as a whole, our results provide evidence that the action of iron contained in chrysotile nanofibers is different from that of a simple iron overload. Such a difference suggests that asbestos fibers are not toxic as simple iron carriers, but rather they could potentiate the redox activity of iron by organizing its ions in specific crystallographic sites having coordination states able to activate free radical generation. This important point has been already stressed in a recent review (*44*), but data supporting this hypothesis are indirect, since until now they have been obtained after drastic physical and chemical modifications of fibers, such as thermal treatment, incubation with oxidizing or reducing agents, coating with iron salts, or "detoxification" with iron chelators (*38*, *44*). These treatments, besides changing iron content and reactivity, can alter the fiber structure (*45*), thus introducing further variables in the interpretation of the results. To our knowledge, this is the first study comparing the effect of fibers specifically designed ab initio with different amounts of iron, without the interference of other variables (such as differences in structure, size, tubular morphology and exposed surface, or physicochemical modifications). Furthermore, EPR data, although obtained in conditions necessarily different from those realized in cellular experiments, suggest that the ability to trigger a Fenton reaction does not seem the main responsible cause of the toxic effects of the fibers; indeed FeNTA was as able as iron-containing fibers to generate HO· radicals in EPR experiments via a Haber−Weiss cycle (*46*) but was not toxic in cellular tests. Our data suggest that cytotoxicity and genotoxicity of iron-containing fibers might be relatable to their ability to trigger production of carbon-centered radicals, which are known to be responsible of peroxidative damage and DNA mutations.

Conclusions

In this study we have compared for the first time the toxicity of chrysotile fibers specifically designed ab initio with different amounts of iron, without the interference of other variables (such as differences in structure, size, tubular morphology and exposed surface, or physicochemical modifications). Our results suggest that the role of iron in asbestos toxicity is more complex than that previously suggested. In other words, iron may behave not simply as a catalytic site generating ROS at the fiber surface but could also influence in a more complex way the interaction between chrysotile fibers and cells. It can induce, for instance, the inhibition of G6PD and the subsequent impairment of the antioxidant defenses of the cells (*14*), leading to a further generation of free radicals and to a more severe cell damage. The mechanism of iron-dependent, asbestos-induced G6PD inhibition is still unclear; we have previously observed in cellular and cell-free systems that GSH prevents the inhibition of G6PD induced by amosite, suggesting the involvement of a redox mechanism (*34*). Furthermore, synthetic stoichiometric and properly loaded chrysotile nanofibers may be proposed as a useful model in studies aimed to investigate the relationship between toxicity and chemical composition of asbestos or to plan the production of much required safe asbestos substitutes (*47*).

Acknowledgment. The research has been carried out with the financial support of Regione Piemonte in the context of a multidisciplinary project "Asbestos Hazard in Western Alps", MIUR (PRIN 2003 and 2005), CNR, Universities of Torino and Bologna (Funds for Selected Research Topics). E.G. and F.T. are recipients of a doctoral fellowship and M.T. of a postdoctoral fellowship from Regione Piemonte. We are grateful to Paolo Spinelli (Laboratorio di Igiene Industriale, Dipartimento di Traumatologia, Ortopedia e Medicina del Lavoro, Università di Torino, Italy) for technical support.

References

(1) Manning, C. B., Vallyathan, V., and Mossman, B. T. (2002) Diseases caused by asbestos: mechanisms of injury and disease development. *Int. Immunopharmacol. 2*, 191−200.

(2) Kamp, D. W., and Weitzman, S. A. (1999) The molecular basis of asbestos induced lung injury. *Thorax 54*, 638−652.
(3) Fubini, B., and Otero-Aréan, C. (1999) Chemical aspects of the toxicity of inhaled mineral dusts. *Chem. Soc. Rev. 28*, 373−381.
(4) Upadhyay, D., and Kamp, D. W. (2003) Asbestos-induced pulmonary toxicity: role of DNA damage and apoptosis. *Exp. Biol. Med. 228*, 650−659.
(5) Schwarz, E. J., and Winer, A. A. (1971) Magnetic properties of asbestos, with special reference to the determination of absolute magnetite contents. *CIM Bull. 64*, 55−59.
(6) De Waele, J. K., Luys, M. J., Vansant, E. F., and Adams, F. C. (1984) Analysis of chrysotile asbestos by LAMMA and Mossbauer spectroscopy: a study of the distribution of iron. *J. Trace Microprobe Tech. 2*, 87−102.
(7) Quinlan, T. R., Marsh, J. P., Janssen, Y. M.W., Borm, P. A., and Mossman, B. T. (1994) Oxygen radicals and asbestos-mediated disease. *Environ. Health Perspect. 102*, 107−110.
(8) Xu, A., Wu, L. J., Santella, R. M., and Hei, T. K. (1999) Role of oxyradicals in mutagenicity and DNA damage induced by crocidolite asbestos in mammalian cells. *Cancer Res. 59*, 5922−5926.
(9) Aust, A. E., and Eveleigh, J. F. (1999) Mechanisms of DNA oxidation. *Proc. Soc. Exp. Biol. Med. 222*, 246−252.
(10) Gilmour, P. S., Brown, D. M., Beswick, P. H., MacNee, W., Rahman, I., and Donaldson, K. (1997) Free radical activity of industrial fibers: role of iron in oxidative stress and activation of transcription factors. *Environ. Health Perspect. 105*, 1313−1317.
(11) Jaurand, M. C. (1997) Mechanisms of fiber-induced genotoxicity. *Environ. Health Perspect. 105*, 1073−1084.
(12) Falini, G., Foresti, E., Lesci, I. G., and Roveri, N. (2002) Structural and morphological characterization of synthetic chrysotile single crystals. *Chem. Commun. 14*, 1512−1513.
(13) Falini, G., Foresti, E., Gazzano, M., Gualtieri, A. F., Leoni, M., Lesci, I. G., and Roveri, N. (2004) Tubular-shaped stoichiometric chrysotile nanocrystals. *Chem. Eur. J. 10*, 3043−3049.
(14) Gazzano, E., Foresti, E., Lesci, I. G., Tomatis, M., Riganti, C., Fubini, B., Roveri, N., and Ghigo, D. (2005) Different cellular responses evoked by natural and stoichiometric synthetic chrysotile asbestos. *Toxicol. Appl. Pharmacol. 206*, 356−364.
(15) Foresti, E., Hochella, M. F., Kornishi, H., Lesci, I. G., Madden, A. S., Roveri, N., and Xu, H. (2005) Morphological and chemical/physical characterization of Fe-doped synthetic chrysotile nanotubes. *Adv. Funct. Mater. 15*, 1009−1016.
(16) Bowes, D. R., and Farrow, C. M. (1997) Major and trace element compositions of the UICC standard asbestos samples. *Am. J. Ind. Med. 32*, 592−594.
(17) Byrd, T. F., and Horwitz, M. A. (1991) Chloroquine inhibits the intracellular multiplication of *Legionella pneumophila* by limiting the availability of iron. A potential new mechanism for the therapeutic effect of chloroquine against intracellular pathogens. *J. Clin. Invest. 88*, 351−357.
(18) Singh, N. P., McCoy, M. T., Tice, R. R., and Schneider, E. L. (1988) A simple technique for quantitation of low levels of DNA damage in individual cells. *Exp. Cell. Res. 175*, 184−191.
(19) Beutler, E. (1971) *Red Cell Metabolism. A Manual of Biochemical Methods*, pp 56−68, Grune & Stratton, New York.
(20) Kinnula, V. L., Aalto, K., Raivio, K. O., Walles, S., and Linnainmaa, K. (1994) Cytotoxicity of oxidants and asbestos fibers in cultured human mesothelial cells. *Free Radical Biol. Med. 16*, 169−176.
(21) Gerard-Monnier, D., Erdelmeier, I., Regnard, K., Moze-Henry, N., Yadan, J. C., and Chaudiere, J. (1998) Reactions of 1-methyl-2-phenylindole with malondialdehyde and 4-hydroxyalkenals. Analytical applications to a colorimetric assay of lipid peroxidation. *Chem. Res. Toxicol. 11*, 1176−1183.
(22) Vandeputte, C., Guizon, I., Genestie-denis, I., Vannier, B., and Lorenzon, G. (1994) A microtiter assay for total glutathione and glutathione disulfide contents in cultured/isolated cells: performance study of a new miniaturized protocol. *Cell Biol. Toxicol. 10*, 415−421.
(23) Riganti, C., Aldieri, E., Bergandi, L., Fenoglio, I., Costamagna, C., Fubini, B., Bosia, A., and Ghigo, D. (2002) Crocidolite asbestos inhibits pentose phosphate pathway and glucose 6-phospate dehydrogenase activity in human lung epithelial cells. *Free Radical Biol. Med. 32*, 938−949.
(24) Fubini, B., Mollo, L., and Giamello, E. (1995) Free radical generation at the solid/liquid interface in iron containing minerals. *Free Radical Res. 23*, 593−614.
(25) Tomatis, M., Prandi, L., Bodoardo, S., and Fubini, B. (2002) Loss of surface reactivity upon heating amphibole asbestos. *Langmuir 18*, 4345−4350.
(26) Fenoglio, I., Prandi, L., Tomatis, M., and Fubini, B. (2001) Free radical generation in the toxicity of inhaled mineral particles: the role of iron speciation at the surface of asbestos and silica. *Redox Rep. 6*, 235−241.
(27) Turci, F., Tomatis, M., Gazzano, E., Riganti, C., Martra, G., Bosia, A., Ghigo, D., and Fubini, B. (2005) Potential toxicity of non-regulated asbestiform minerals: balangeroite from Western Alps. Part 2: oxidant activity of the fibres. *J. Toxicol. Environ. Health 68*, 21−39.
(28) Bui, M. H., Sauty, A., Collet, F., and Leuenberger, P. (1992) Dietary vitamin C intake and concentrations in the body fluids and cells of male smokers and nonsmokers. *J. Nutr. 122*, 312−316.
(29) Anderegg, G. (1982) Critical survey of stability constants of NTA complexes. *Pure Appl. Chem. 54*, 2693−2758.
(30) Martell, A. E., and Smith, R. M. (1977) *Critical Stability Constants*, Plenum, New York.
(31) Kamp, D., Panduri, V., Weitzman, S., and Chandel, N. (2002) Asbestos-induced alveolar epithelial cell apoptosis: role of mitochondrial dysfunction caused by iron-derived free radicals. *Mol. Cell. Biochem. 234−235*, 153−160.
(32) Shukla, A., Stern, M., Fukagawa, N. K., Taatjes, D. J., Sawyer, D., Van Houten, B,. and Mossman, B. T. (2003) Asbestos induces mitochondrial DNA damage and dysfunction linked to the development of apoptosis. *Am. J. Physiol. Lung Cell. Mol. Physiol. 285*, L1018−1025.
(33) Panduri, V., Weitzman, S. A., Chandel, N. S., and Kamp, D. W. (2004) Mitochondrial-derived free radicals mediate asbestos-induced alveolar epithelial cell apoptosis. *Am. J. Physiol. Lung Cell. Mol. Physiol. 286*, L1220−L1227.
(34) Riganti, C., Aldieri, E., Bergandi, L., Tomatis, M., Fenoglio, I., Costamagna, C., Fubini, B., Bosia, A., and Ghigo, D. (2003) Long and short fiber amosite asbestos alters at a different extent the redox metabolism in human lung epithelial cells. *Toxicol. Appl. Pharmacol. 193*, 106−115.
(35) Wefers, H., and Sies, H. (1983) Hepatic low-level chemiluminescence during redox cycling of menadione and the menadione−glutathione conjugate: relation to glutathione and NAD(P)H:quinone reductase (DT-diaphorase) activity. *Arch. Biochem. Biophys. 224*, 568−578.
(36) Gaetani, D. G., Parker, J. C., and Kirkman, H. N. (1974) Intracellular restraint: a new basis for the limitation in response to oxidative stress in human erythrocytes containing low activity variants of glucose-6-phosphate dehydrogenase. *Proc. Natl. Acad. Sci. U.S.A. 71*, 3584−3587.
(37) Fang, R., and Aust, A. E. (1997) Induction of ferritin synthesis in human lung epithelial cells treated with crocidolite asbestos. *Arch. Biochem. Biophys. 340*, 369−375.
(38) Gulumian, M. (2005) An update on the detoxification processes for silica particles and asbestos fibers: successes and limitations. *J. Toxicol. Environ. Health, Part B 8*, 453−483.
(39) Inoue, S., and Kawanishi, S. (1987) Hydroxyl radical production and human DNA damage induced by ferric nitrilotriacetate and hydrogen peroxide. *Cancer Res. 47*, 6522−6527.
(40) Bacon, B. R., Tavill, A. S., Brittenham, G. M., Park, C. H., and Recknagel, R. O. (1983) Hepatic lipid peroxidation in vivo in rats with chronic iron overload. *J. Clin. Invest. 71*, 429−439.
(41) Glei, M., Latunde-Dada, G. O., Klinder, A., Becker, Th. W., Hermann, U., Voigt, K., and Pool-Zobel, B. L. (2002) Iron-overload induces oxidative DNA damage in the human colon carcinoma cell line HT29 clone 19A. *Mutat. Res. 519*, 151−161.
(42) Carini, R., Parola, M., Dianzani, M. U., and Albano, E. (1992) Mitochondrial damage and its role in causing hepatocyte injury during stimulation of lipid peroxidation by iron nitriloacetate. *Arch. Biochem. Biophys. 297*, 110−118.
(43) Matos, H. R., Di Mascio, P., and Medeiros, M. H. G. (2000) Protective effect of lycopene on lipid peroxidation and oxidative DNA damage in cell culture. *Arch. Biochem. Biophys. 383*, 56−59.
(44) Shukla, A., Gulumian, M., Hei, T. K., Kamp, D., Rahman, Q., and Mossman, B. T. (2003) Multiple roles of oxidants in the pathogenesis of asbestos-induced diseases. *Free Radical Biol. Med. 34*, 1117−1129.
(45) Gold, J., Amandusson, H., Krozer, A., Kasemo, B., Ericsson, T., Zanetti, G., and Fubini, B. (1997) Chemical characterization and reactivity of iron chelator-treated amphibole asbestos. *Environ. Health Perspect. 105 (Suppl. 5*), 1021−1030.
(46) Halliwell, B., and Gutteridge, J. M.C. (1984) Oxygen toxicity, oxygen radicals, transition metals and disease. *Biochem. J. 219*, 1−14.
(47) Bernstein, D., Castranova, V., Donaldson, K., Fubini, B., Hadley, J., Hesterberg, T., Kane, A., Lai, D., McConnell, E. E., Muhle, H., Oberdorster, G., Olin, S., and Warheit, D. B. (2005) Testing of fibrous particles: short-term assays and strategies. *Inhalation Toxicol. 17*, 1−41.

TX600354F